Plastic waste as a feedstock for solar-driven H_2 generation

Taylor Uekert,[a] Moritz F. Kuehnel,[a,b]* David W. Wakerley,[a] and Erwin Reisner[a]*

a. Christian Doppler Laboratory for Sustainable SynGas Chemistry, Department of Chemistry, University of Cambridge, Lensfield Road, Cambridge CB2 1EW, UK
b. Department of Chemistry, Swansea University, College of Science, Singleton Park SA2 8PP, UK

* Corresponding authors: E.R. reisner@ch.cam.ac.uk, M.F.K m.f.kuehnel@swansea.ac.uk

Abstract: Solar-driven photoreforming of plastics offers a simple and low-energy means to turn waste into H_2. Here, we report the efficient photoreforming of three commonly produced polymers – polylactic acid, polyethylene terphthalatate (PET) and polyurethane – using inexpensive CdS/CdO_x quantum dots in alkaline aqueous solution. This process operates under ambient temperature and pressure, generates pure H_2 and converts the waste polymer into high-value organic products such as formate, acetate and pyruvate. We further validate the real-world applicability of the system by successfully converting a PET water bottle to H_2. This is the first demonstration of visible light-driven, noble metal-free photoreforming of plastic.

Broader Context

More than 8 billion tons of plastic have been produced since 1950, and roughly one million plastic bottles are purchased worldwide every minute. As landfills near capacity and concerns rise over plastic pollution in the oceans, it is becoming increasingly apparent that new methods for reusing polymers are desperately needed. Solar-driven reforming is a novel approach that enables the conversion of waste plastic into an energy source: H_2 fuel. This process only requires sunlight and a suitable photocatalyst. We report the visible-light driven reforming of three common polymers (including a PET water bottle) with a precious metal-free photocatalyst. This serves as proof-of-concept for the ability of photo-reforming to address two global challenges: plastic waste alleviation and renewable fuel production.

Main text

Plastics are ideal for a vast range of applications due to their low cost and versatile properties, but their use also contributes to an ever-expanding disposal challenge. Eight million tons of plastic enter the oceans every year, and marine plastic pollution is predicted to outweigh the fish in the oceans by 2050.[1] Although recycling is increasingly prevalent, a third of all plastics are still too small or complex to recover economically.[2,3] The severity and complexity of this waste challenge means that additional methods for recycling or reusing polymers are urgently needed.

A potential solution is to use plastic waste as a feedstock for H_2 generation. Over 50 million tons of H_2 are produced annually worldwide for use in the agricultural, chemical and pharmaceutical industries.[4] H_2 is also a promising renewable energy carrier,[5,6] yet 96% of the global H_2 supply is currently generated via steam reforming of fossil fuels.[7] Pyrolysis of waste plastics has been proposed as a replacement for this non-renewable process, but while it achieves H_2 yields of 80-90%, it still requires significant energy input (500-800 °C) and releases greenhouse gases (~12 kg CO_2 per 1 kg H_2).[8–11]

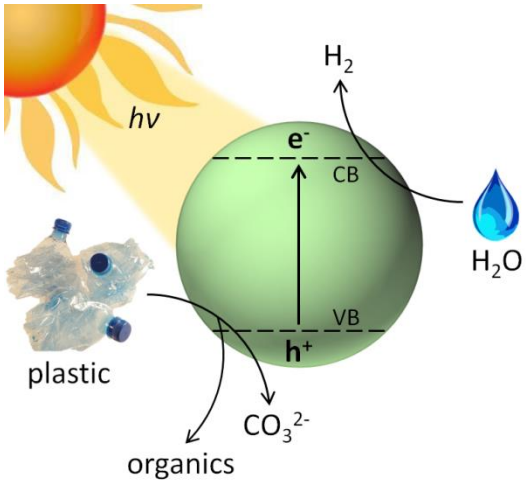

Figure 1. Diagram of the polymer photoreforming process with a CdS/CdO_x quantum dot photocatalyst in aqueous solution.

We propose ambient-temperature photoreforming (PR) of plastic waste as an alternative. Photoreforming requires four components – a photocatalyst, substrate, sunlight and water – to generate H_2 at ambient pressure and temperature (Fig. 1). Electrons are excited to the conduction band (CB) of the photocatalyst by sunlight, and reduce water to H_2. The resulting holes in the valence band (VB) of the photocatalyst oxidise the substrate to smaller organic molecules that remain in solution.

PR of simple alcohols has been researched extensively,[12,13] but these processed substrates are too costly for industrial H_2 production. Freely-available substrates such as waste plastics are therefore an attractive alternative, but are more challenging to reform due to their complex structures, low water solubilities and non-biodegradability. PR of plastics is thus limited to a single example of TiO_2 producing low yields of H_2 and CO_2 from polyethylene (PE), polyvinyl alcohol and polyvinyl chloride (PVC).[14] In addition to its poor activity, this system was constrained by its use of an expensive platinum co-catalyst and reliance on UV irradiation.

Here, we implement a CdS/CdO_x quantum dot (QD) photocatalyst in alkaline aqueous solution to photoreform plastics. We demonstrate for the first time that pure H_2 can be evolved from polylactic acid (PLA), polyethylene terephthalate (PET), polyurethane (PUR) and a PET water bottle. Simultaneously, the polymer is also valorised to organic products. Plastic PR with CdS offers a unique approach towards mitigating waste and generating H_2 and organic chemicals in a visible light-driven process.

CdS has a bulk band gap of 2.4 eV that allows for visible light absorption, and band positions (CB −0.5 V vs. NHE, VB +1.9 V vs. NHE) favourable for the PR half-reactions outlined above.[15] It also does not require a co-catalyst to reduce water to H_2, in contrast to TiO_2 and many other photocatalytic systems.[16,17] Despite its toxicity, Cd is inexpensive and commercially employed for energy conversion applications in CdTe photovoltaics.[18] In this study, we used a CdS/CdO_x QD photocatalyst.[19,20] When CdS QDs (diameter ~5 nm, Table S1, Fig. S1a, λ_{max} ~450 nm, Fig. S2a) are dispersed in aqueous NaOH, they form a thin Cd oxide/hydroxide shell (CdO_x) that prevents photocorrosion.[20,21] Ligand-free QDs were utilised with most substrates as their exposed surfaces tend to correlate with superior catalytic performance (Table S2).[22,23] Oleic acid-capped QDs were used only with PET as they offered slightly

higher efficiencies (Table S2), potentially due to a hydrophobic effect favouring substrate-QD interaction.

A variety of polymers were tested for PR over CdS/CdO_x. Polyvinyl pyrrolidone, polyethylene glycol, PE, PVC, polymethyl methacrylate, polystyrene and polycarbonate all produced small quantities of H_2 (Table S3). PLA, PET and PUR exhibited higher activities and were therefore selected for further study. PLA is a biodegradable polymer used for biomedical purposes, 3D printing, and environmentally-friendly packaging.[24] Since PLA is a potential replacement for PET and polystyrene,[25] it should ideally be utilised at the end of its life cycle rather than merely degraded. PET accounts for 9% of global plastic production and is used in packaging. While it is recycled to a certain extent, the resulting material is often not reused because of its inferior properties.[3] Novel recycling methods such as PET-degrading enzymes[26] are promising in their ability to digest plastic, but unlike PR, are unable to produce fuel or other useful products. PUR is found in insulation and vehicle components, and is very challenging to recycle due to its composite nature.[27]

In a typical experiment, commercially available polymers were ground to powders, suspended in 10 M aq. NaOH in the presence of CdS/CdO_x QDs under N_2 (atmospheric pressure), and exposed to simulated solar light (AM 1.5G, 100 mW cm^{-2}) at 25 °C (see ESI for details). All experimental conditions, including QD, NaOH and substrate concentrations, were optimised for maximum H_2 generation (Table S2, S4). PR of PLA, PET and PUR generates H_2 with activities of 64.3 ± 14.7, 3.42 ± 0.87, and 0.85 ± 0.28 $mmol_{H2}\ g_{CdS}^{-1}\ h^{-1}$, respectively. H_2 production continues beyond 22 h to totals of 3.09 ± 0.15, 0.21 ± 0.04, and 0.04 ± 0.01 $mmol_{H2}\ g_{substrate}^{-1}$ (Fig. S3, Table S5, S6). These activities correspond to external quantum yields of 15.0 ± 0.7% for PLA, 3.74 ± 0.34% for PET, and 0.14 ± 0.03% for PUR at λ = 430 nm (Table S7). All values are background-corrected by activity without substrates (Table S8), and no H_2 is detected without QDs or light (Table S9). PR proceeds efficiently without UV irradiation (λ > 400 nm), indicating that the catalyst utilises visible light (Table S9). Mass spectrometry in deuterated and non-deuterated solvent confirms that the generated H_2 originates from water rather than the substrate (Fig. S4a). Transmission electron microscopy and UV-Vis spectroscopy (Fig. S1, S2) indicate that the CdS/CdO_x QDs undergo minor aggregation during PR, a known phenomenon for CdS QDs.[19]

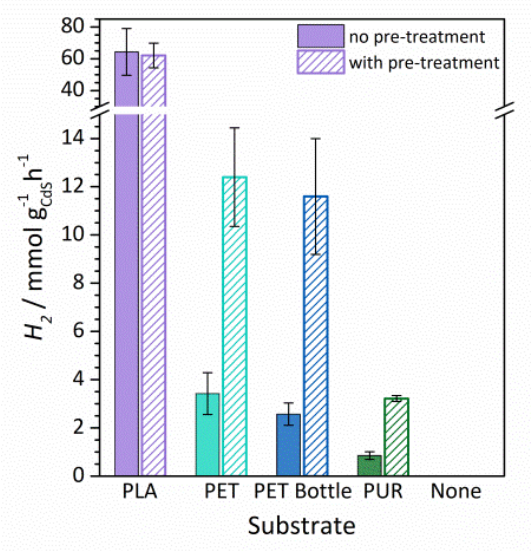

Figure 2. Photoreforming of polymers to H_2 using CdS/CdO_x QDs (1 nmol) under simulated solar light (4 h, AM 1.5G, 100 mW cm^{-2}, 25 °C). Conditions: powdered plastic (50 mg mL^{-1} PLA, 25 mg mL^{-1} PET, PET bottle or PUR) freshly prepared (no pre-treatment) or pre-treated in 10 M aq. NaOH (2 mL).

Importantly, these activities obtained from freely-available waste plastic are comparable to CdS-based PR of more expensive substrates, such as furfural on Ni/CdS (3.9 $mmol_{H2}$ g_{cat}^{-1} h^{-1}),[28] lactic acid on NiS/CdS (7.3 $mmol_{H2}$ g_{cat}^{-1} h^{-1}),[29] and glucose on MoS_2/CdS (55 $mmol_{H2}$ g_{cat}^{-1} h^{-1}).[30] They are also superior to those reported for the only previous example of plastic PR. 5% Pt/TiO_2 in 5 M aq. NaOH gave rates of 0.031 and 0.015 $mmol_{H2}$ g_{cat}^{-1} h^{-1} with PE and PVC,[14] whereas CdS/CdO_x shows activities of up to 8.5 and 17 times higher (Table S3).

For a more direct comparison, 5% Pt/TiO_2 in 10 M aq. NaOH was also studied for PR of PLA and PET, yielding 0.011 ± 0.004 and 0.074 ± 0.029 $mmol_{H2}$ g_{cat}^{-1} h^{-1}, respectively (Table S10). These rates are significantly lower (over 50 times) than those obtained with CdS/CdO_x QDs under identical conditions, and require the use of an expensive co-catalyst (no H_2 is observed without Pt). Other Cd-free catalysts such as ZnSe QDs have also been tested, but do not demonstrate H_2 evolution. PR with CdS/CdO_x QDs is thus characterised by unique benefits including visible light absorption, lack of co-catalysts, and rapid oxidation of complex substrates.

To further enhance the PR activity, we developed a simple pre-treatment comprising stirring the substrate in 10 M aq. NaOH for 24 h at 40 °C in the dark followed by centrifugation and use of only the supernatant as the photocatalysis substrate. Under optimised conditions, pre-treatment improves the activity of the PR system by four times for both PET and PUR, to 12.4 ± 2.0 and 3.22 ± 0.13 $mmol_{H2}$ g_{CdS}^{-1} h^{-1}, respectively (Fig. 2, Table S3, S11). Alkaline hydrolysis is a common technique for converting PET[31–33] and, to a lesser extent, PUR[34] into monomers which can then be re-used. Here, pre-treatment initiates hydrolysis, releasing monomers into solution which can be more rapidly photoreformed. For example, the ^{1}H-NMR spectrum of pre-treated PET shows a significant enhancement in peak intensity in comparison to that of untreated PET (Fig. S5a). Untreated samples also hydrolyse, but at slower initial rates; hence their lower activities (Fig. 2).

In addition, removal of undissolved polymer by centrifugation reduces the absorbance and scattering of the PR solution (Fig. S5c), allowing more photons to reach the QDs and thus improving efficiency. Accordingly, pre-treatment without centrifugation does not enhance PR performance as significantly (Table S11). PLA is unaffected by pre-treatment since it already dissolves readily in NaOH (Fig. S5b, S5c). Pre-treatment facilitates PR of complex polymers to H_2 and is only possible because CdS/CdO_x QDs, unlike many photocatalysts, can operate under highly alkaline conditions.

Controlling the oxidation half-reaction is crucial in order to generate high-value organic products instead of CO_2. We used ^{1}H-NMR spectroscopy to analyse the reaction mixtures and identify the organic oxidation products. Since chemical shifts can be significantly altered in strongly alkaline solution, all peak assignments were verified by adding authentic samples (Fig. S6) to the reaction mixtures and examining the ^{1}H-NMR spectra for peak matching.

PLA in NaOH hydrolyses to sodium lactate (peak *a*, *b*), which is oxidised to pyruvate[35] or an alkalinity-induced pyruvate-based compound (*c*) during PR (Fig. 3a, S7).

PET (Fig. 3b) undergoes hydrolysis to terephthalate (*a*) ethylene glycol (*b*), and isophthalate (*d*, *e*, *f*), while photo-oxidation produces formate (*c*), glycolate (*g*), ethanol (*h*, *m*), acetate (*i*) and lactate (*l*). Similar PET oxidation products have been previously reported.[36,37] Isophthalate is likely added during PET synthesis, as it is already visible prior to irradiation (Fig. S5a). Its relatively high intensity in comparison to terephthalate is due to its higher solubility in basic conditions.[38] Peaks *j* and *k* have not been identified; their appearance in pre-treated PET (Fig. S5a inset) suggests that they may be linkers or fillers in the polymer.

PR of ethylene glycol yields H_2 at a rate of 6.83 ± 0.43 $mmol_{H2}$ g_{CdS}^{-1} h^{-1} and displays the same oxidation products as PET (Table S3, Fig. S8). In contrast, PR of terephthalic acid does not produce H_2 (Table S3), suggesting that the oxidation products of PET originate exclusively from its aliphatic component. Terephthalic acid, a valuable material for chemical synthesis, precipitates as its disodium salt[39] from the PR solution and could thus be easily isolated (Fig. S9).

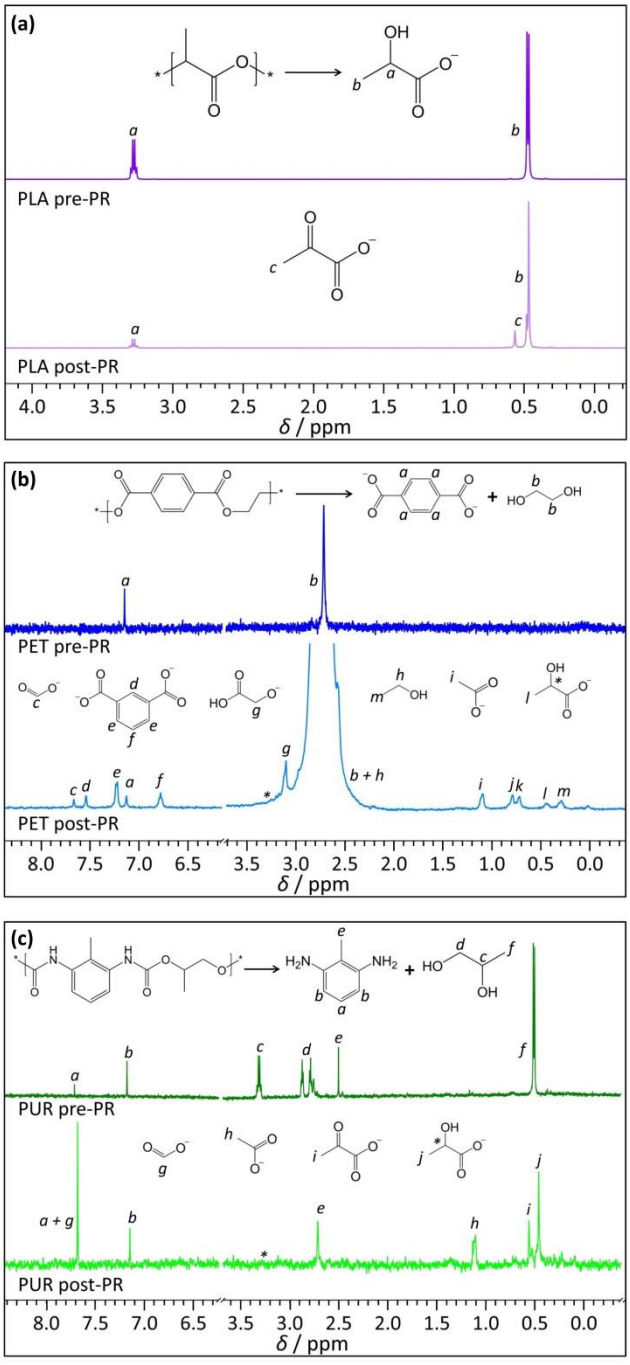

Figure 3. ^{1}H-NMR spectra of **(a)** PLA, **(b)** PET, and **(c)** PUR before (pre-PR) and after (post-PR) 24 h irradiation (AM 1.5G, 100 mW cm^{-2}, 25 °C) with CdS/CdO_x QDs (1 nmol) in 10 M NaOD in D_2O (2 mL).

PUR (Fig. 3c) first hydrolyses to aromatic (2,6-diaminotoluene, *a*, *b*, *e*) and aliphatic (propylene glycol or similar, *c*, *d*, *f*) components. In agreement with the literature,[37,40] the aromatic constituent remains intact during PR (no H_2 production, Table S3), whereas the aliphatic components are photo-oxidised to formate (*g*), acetate (*h*), pyruvate (*i*) and lactate (*j*).

Conversion efficiencies were studied by performing PR to completion at varying, low substrate-to-catalyst ratios (Table 1, S12, Fig. S10). Extrapolating the produced H_2 to infinite catalyst loading gives the limiting H_2 yield (N_{lim}).[41,42] Conversion is calculated by dividing N_{lim} by the theoretical H_2 yield, $N_{100\%}$ (determined from Eq. 2, 4 and 6 for PLA, PET and PUR, respectively). Note that Eq. 4 and 6 assume that only the aliphatic components of PET and PUR are further oxidised to release H_2, as determined in the above NMR analysis. While the conversions of PLA and PET follow the expected linear trend over the entire range of substrate concentrations (0.1-0.5 mg mL^{-1}), PUR shows much higher conversions at low concentrations due to its poor solubility.

PLA:

hydrolysis: $C_3H_4O_2 + H_2O \xrightarrow{NaOH} C_3H_6O_3$ [Eq. 1]

PR: $C_3H_6O_3 + 3\ H_2O \xrightarrow{hv,\ CdS} \mathbf{6\ H_2} + 3\ CO_2$ [Eq. 2]

PET:

hydrolysis: $C_{10}H_8O_4 + 2\ H_2O \xrightarrow{NaOH} C_8H_6O_4 + C_2H_6O_2$ [Eq. 3]

PR: $C_2H_6O_2 + 2\ H_2O \xrightarrow{hv,\ CdS} \mathbf{5\ H_2} + 2\ CO_2$ [Eq. 4]

PUR:

hydrolysis: $C_{12}H_{14}N_2O_4 + 2\ H_2O \xrightarrow{NaOH} C_7H_{10}N_2 + C_3H_8O_2 + 2\ CO_2$ [Eq. 5]

PR: $C_3H_8O_2 + 4\ H_2O \xrightarrow{hv,\ CdS} \mathbf{8\ H_2} + 3\ CO_2$ [Eq. 6]

Table 1. Limiting yield (N_{lim}), theoretical yield ($N_{100\%}$, calculated from Eqs. 2, 4, 6), and conversion of PLA, PET and PUR (24 h PR, 1 nmol $CdSCdO_x$ QDs, AM 1.5G, 100 mW cm^{-2}, 25 °C; Fig. S10 and Table S12).

Substrate	N_{lim} ± σ ($mol_{H2}\ mol_{sub}^{-1}$)	$N_{100\%}$ ($mol_{H2}\ mol_{sub}^{-1}$)	Conversion ± σ (%)
PLA	2.33 ± 0.24	6.0	38.8 ± 4.0
PET	0.83 ± 0.05	5.0	16.6 ± 1.0
PUR	1.80 ± 0.27	8.0	22.5 ± 3.4

Despite the high initial activity, overall conversion remains below 40% for all polymers. This is primarily because the polymers are not completely mineralised to CO_2, unlike in the ideal equations above. No CO_3^{2-} is detected in the ^{13}C-NMR spectra of the PR solutions (Fig. S7), and mass spectrometry confirms that no gaseous CO_2 is released (Fig. S4b). Instead, the polymers are partially oxidised to organic molecules, many of which undergo slow PR (Table S3) and remain in solution. Although this effect lowers H_2 production, it prevents the discharge of a greenhouse gas and allows for the beneficial accumulation of high-value products in solution. Furthermore, PR of PLA in the presence of terephthalic acid exhibits suppressed H_2 evolution (Table S13). This suggests that terephthalic acid acts as an inhibitor, likely by obstructing substrate binding sites on the CdS/CdO_x surface. Similar effects are expected from the other carboxylic products. Deactivation of the catalyst is not observed as activity always resumes upon substrate re-addition (Table S13).

Finally, we studied PR of a PET water bottle to demonstrate the real-world applicability of our system. It is crucial to test real plastic samples, as they typically contain additional fillers, cross-linkers or antioxidants that could make PR more challenging. Fig. 4 shows continuous H_2 generation from the water bottle over the course of 6 days, with an activity of up to 4.13 ± 0.40 $mmol_{H2}\ g_{CdS}^{-1}\ h^{-1}$ (Table S6), external quantum yield of 2.17 ± 0.38% (Table S7), and conversion of 5.15 ± 0.72% (calculated from Eq. 4). Pre-treatment provides an initial improvement in H_2 evolution rate; this advantage slows over time as polymer hydrolysis proceeds in the untreated sample.

Scanning electron microscopy reveals that the surface of the untreated bottle erodes during photoreforming, from a smooth morphology to one featuring pits and grains (Fig. S11). During this PR process, a variety of organic molecules, including glyoxylate, methylglyoxal and methanol in addition to those seen in pure PET, are also produced (^1H-NMR, Fig. S12). These results not only indicate that CdS system remains stable after 6 days of continuous PR, but also clearly demonstrate the applicability of PR to real plastic waste.

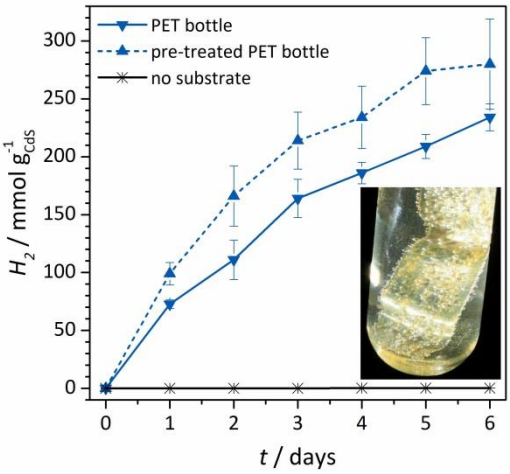

Figure 4. Long-term photoreforming of a PET bottle to H_2 using CdS/ CdO_x QDs (1 nmol) under simulated sunlight (6 days, AM 1.5G, 100 mW cm^{-2}, 25 °C). Conditions: ground PET bottle (25 mg mL^{-1}) freshly prepared or pre-treated in 10 M aq. NaOH (2 mL). Inset: photograph of a PET bottle sample; H_2 bubbles are visible on the plastic surface.

In this work, we have generated H_2 and organics by photoreforming a variety of widely-produced plastics, including polylactic acid, polyethylene terephthalate and polyurethane, over CdS/CdO_x QDs. Our system efficiently utilises visible light and does not require expensive precious metals. Future work will improve upon this proof-of-concept system by identifying alternative catalysts and methods for further enhancing activities. Plastic waste is often difficult, inefficient or inconvenient to re-use. Photoreforming utilises this abundant resource in a simple process that generates valuable H_2 and organics. As such, it is a technique capable of simultaneously addressing the global challenge of plastic pollution and implementing renewable H_2 generation.

Conflicts of interest

A patent application covering this work has been filed by Cambridge Enterprise (PCT/EP2017/080371) that names M.F.K., D.W.W. and E.R. as inventors.

Acknowledgements

This work was supported by the Christian Doppler Research Association (Austrian Federal Ministry of Science, Research and Economy and the National Foundation for Research, Technology and Development), OMV Group, and EPSRC (NanoDTC studentship EP/L015978/1 to T.U., DTA studentship to D.W.W. and IAA Follow-on fund to M.F.K. and E.R.). We thank Kristian Dalle for assistance in recording mass spectra, Constantin Sahm for assistance with transmission electron microscopy, Hatice Kasap and Julien Warnan for discussions and Jacqui Jones for photography.

References

1 E. MacArthur, *Science*, 2017, **358**, 843.
2 R. Geyer, J. R. Jambeck and K. L. Law, *Sci. Adv.*, 2017, **3**, e1700782.
3 J. M. Garcia and M. L. Robertson, *Science*, 2017, **358**, 870–872.
4 DOE, *Report of the Hydrogen Production Expert Panel: A Subcommittee of the Hydrogen & Fuel Cell Technical Advisory Committee*, Washington, D.C., 2013.
5 International Energy Agency, *Tracking Clean Energy Progress 2015: Energy Technology Perspectives 2015 Excerpt IEA Input to the Clean Energy Ministerial*, Paris, 2015.
6 P. Cai, Y. Li, G. Wang and Z. Wen, *Angew. Chem. Int. Ed.*, 2018, **57**, 3910–3915.
7 A. Iulianelli, S. Liguori, J. Wilcox and A. Basile, *Catal. Rev.*, 2016, **58**, 1–35.
8 P. L. Spath and M. K. Mann, *Life Cycle Assessment of Hydrogen Production via Natural Gas Steam Reforming*, Golden, 2001.
9 S. Czernik and R. J. French, *Energy & Fuels*, 2006, **20**, 754–758.
10 G. Lopez, A. Erkiaga, M. Artetxe, M. Amutio, J. Bilbao and M. Olazar, *Ind. Eng. Chem. Res.*, 2015, **54**, 9536–9544.
11 I. Barbarias, G. Lopez, J. Alvarez, M. Artetxe, A. Arregi, J. Bilbao and M. Olazar, *Chem. Eng. J.*, 2016, **296**, 191–198.
12 M. Kuehnel and E. Reisner, *Angew. Chem. Int. Ed.*, 2018, **57**, 3290-3296.
13 A. V. Puga, *Coord. Chem. Rev.*, 2016, **315**, 1–66.
14 T. Kawai and T. Sakata, *Chem. Lett.*, 1981, 81–84.
15 Y. Xu, Y. Huang and B. Zhang, *Inorg. Chem. Front.*, 2016, **3**, 591–615.
16 V. W. Lau, D. Klose, H. Kasap, F. Podjaski, M. C. Pignié, E. Reisner, G. Jeschke and B. V. Lotsch, *Angew. Chem. Int. Ed.*, 2017, **56**, 510–514.
17 P. Cai, J. Huang, J. Chen and Z. Wen, *Angew. Chem. Int. Ed.*, 2017, **56**, 4858–4861.
18 B. M. Basol and B. McCandless, *J. Photonics Energy*, 2014, **4**, 040996.
19 M. F. Kuehnel, D. W. Wakerley, K. L. Orchard and E. Reisner, *Angew. Chem. Int. Ed.*, 2015, **54**, 9627–9631.
20 D. W. Wakerley, M. F. Kuehnel, K. L. Orchard, K. H. Ly, T. E. Rosser and E. Reisner, *Nat. Energy*, 2017, **2**, 17021.
21 D. Wakerley, K. Ly, N. Kornienko, K. Orchard, M. Kuehnel and E. Reisner, *Chem. A Eur. J.*, 2018, **24**.
22 C. M. Chang, K. L. Orchard, B. C. M. Martindale and E. Reisner, *J. Mater. Chem. A*, 2016, **4**, 2856–2862.
23 M. F. Kuehnel, C. D. Sahm, G. Neri, J. R. Lee, K. L. Orchard, A. J. Cowan and E. Reisner, *Chem. Sci.*, 2018, **9**, 2501–2509.
24 A. C. Albertsson and M. Hakkarainen, *Science*, 2017, **358**, 872–873.
25 M. A. Hillmyer, *Science*, 2017, **358**, 868–870.
26 H. P. Austin, M. D. Allen, B. S. Donohoe, N. A. Rorrer, F. L. Kearns, R. L. Silveira, B. C. Pollard, G. Dominick, R. Duman, K. El Omari, V. Mykhaylyk, A. Wagner, W. E. Michener, A. Amore, M. S. Skaf, M. F. Crowley, A. W. Thorne, C. W. Johnson, H. L. Woodcock, J. E. Mcgeehan and G. T. Beckham, *Proc. Natl. Acad, Sci.*, 2018, 10.1073/pnas.1718804115.
27 EUROPUR, *Flexible Polyurethane Foam in Mattresses and Furniture: an Overview of Possible End of Life Solutions*, Brussels, 2016.
28 G. Han, Y. H. Jin, R. A. Burgess, N. E. Dickenson, X. M. Cao and Y. Sun, *J. Am. Chem. Soc.*, 2017, **139**, 15584–15587.
29 W. Zhang, Y. Wang, Z. Wang, Z. Zhong and R. Xu, *Chem. Commun.*, 2010, **46**, 7631.
30 C. Li, H. Wang, J. Ming, M. Liu and P. Fang, *Int. J. Hydrogen Energy*, 2017, **42**, 16968–16978.
31 C.-Y. Kao, W.H. Cheng and B.Z. Wan, *J. Appl. Polym. Sci.*, 1998, **70**, 1939–1945.
32 D. Carta, G. Cao and C. D'Angeli, *Environ. Sci. Pollut. Res.*, 2003, **10**, 390–394.
33 S. Kumar and C. Guria, *J. Macromol. Sci. Part A*, 2005, **42**, 237–251.
34 K. M. Zia, H. N. Bhatti and I. Ahmad Bhatti, *React. Funct. Polym.*, 2007, **67**, 675–692.
35 T. Tsujino, S. Ohigashi, S. Sugiyama, K. Kawashiro and H. Hayashi, *J. Mol. Catal.*, 1992, **71**, 25–35.
36 H. Yue, Y. Zhao, X. Ma and J. Gong, *Chem. Soc. Rev.*, 2012, **41**, 4089–4380.
37 W. J. Rossiter, P. W. Brown and M. Godette, *Sol. Energy Mater.*, 1983, **9**, 267–279.
38 *The MAK Collection Part I: MAK Value Documentations, Vol. 25*, WILEY-VCH, Weinheim, 2009.
39 G. P. Karayannidis, A. P. Chatziavgoustis and D. S. Achilias, *Adv. Polym. Technol.*, 2002, **21**, 250–259.
40 W. L. Evans, *J. Am. Chem. Soc.*, 1923, **45**, 171–176.
41 T. Shiragami, T. Tomo, H. Tsumagari, Y. Ishii and M. Yasuda, *Catalysts*, 2012, **2**, 56–67.
42 T. Shiragami, T. Tomo, H. Tsumagari, R. Yuki, T. Yamashita and M. Yasuda, *Chem. Lett.*, 2012, **41**, 29–31.